Computer-Aided Diagnosis of Hepatic Fibrosis: Preliminary Evaluation of MRI Texture Analysis Using the Finite Difference Method and an Artificial Neural Network

Hiroki Kato[1]
Masayuki Kanematsu[1,2]
Xuejun Zhang[3]
Masanao Saio[4]
Hiroshi Kondo[1]
Satoshi Goshima[1]
Hiroshi Fujita[5]

OBJECTIVE. The purpose of our study was to preliminarily evaluate the usefulness of a computer algorithm analysis using the finite difference method and an artificial neural network to diagnose hepatic fibrosis with MR images.

MATERIALS AND METHODS. Liver parenchymal textures on the MR images of 52 patients who underwent partial hepatectomy were processed by the computer algorithm and reviewed by two radiologists. The texture features using the finite difference method were processed by an artificial neural network program containing a three-layer learning algorithm of the back propagation, composed of a seven-unit input layer, a six-unit hidden layer, and a one-unit output layer. The radiologists assigned confidence levels for the presence of hepatic fibrosis. Degrees of hepatic fibrosis were determined semiquantitatively by a pathologist. Algorithm outputs and radiologists' interpretations were correlated with degrees of fibrosis using Spearman's rank correlation analysis, and diagnostic performances were evaluated using receiver operating characteristic curve analysis.

RESULTS. By the computer algorithm, the A_z (area under the curve) value was greater for gadolinium-enhanced equilibrium phase images ($A_z = 0.801$) than for T1-weighted ($A_z = 0.597$) or T2-weighted ($A_z = 0.525$) images ($p < 0.05$), and the outputs of equilibrium phase images showed a moderate correlation ($r = 0.502$, $p = 0.001$) with the pathologic grades. By the radiologists' interpretations, the A_z value for all images combined ($A_z = 0.715$) was greater than that of portal venous phase images ($A_z = 0.503$) ($p < 0.05$), and the confidence levels of all images combined were moderately correlated ($r = 0.473$, $p = 0.002$) with pathologic grades.

CONCLUSION. Computer algorithm analysis of equilibrium phase images was found to reflect the degree of fibrosis most accurately. MR image texture analysis performed using the computer algorithm was found to have a potential usefulness for the diagnosis of hepatic fibrosis.

Keywords: computer-aided diagnosis, fibrosis, liver, MRI

DOI:10.2214/AJR.07.2070

Received August 28, 2006; accepted after revision February 22, 2007.

Supported in part by the Health and Labour Sciences Research Grants for Third Term Comprehensive Control Research for Cancer from the National Cancer Center Hospital, Tokyo, Japan.

[1]Department of Radiology, Gifu University School of Medicine, 1-1 Yanagido, Gifu 501-1194, Japan. Address correspondence to H. Kato (hkato@gifu-u.ac.jp).

[2]Department of Radiology Services, Gifu University Hospital, Gifu, Japan.

[3]College of Computer Science and Information Engineering, Guangxi University, Nanning City, Guangxi, P. R. China.

[4]Department of Immunopathology, Gifu University Graduate School of Medicine, Gifu, Japan.

[5]Department of Information Science, Faculty of Engineering, Gifu University, Gifu, Japan.

AJR 2007; 189:117–122

0361–803X/07/1891–117

A remarkable increase in the incidence of primary liver tumors has occurred in the developed Western world and in Asia and Africa over the past few decades, which could be a consequence of hepatitis C virus acquisition during the 1960s and 1970s. Patients with chronic viral hepatitis are at great risk of developing complications such as hepatocellular carcinoma, cirrhosis, and resulting liver failure [1, 2]. Hepatocellular carcinoma is the most frequent and life-threatening complication, particularly in patients who are positive for hepatitis C virus [3]. The degree of liver fibrosis is a critical predictive factor for the occurrence of hepatocellular carcinoma [4], and the cumulative incidence of hepatocellular carcinoma was significantly higher in patients with severe fibrosis (F3 and F4) than in those with no or mild fibrosis (F0 to F2) [5]. Thus, the early detection and accurate staging of hepatic fibrosis or cirrhosis has become a critical issue in radiology practice.

Regenerative nodules and surrounding fibrosis become prominent as cirrhosis progresses, and the computerized recognition of the degree of a reformed parenchymal texture in cirrhosis has the potential to assess the degree of cirrhosis. MRI has a great advantage for the depiction of hepatic parenchymal multinodularity in cirrhosis because of its high sensitivity for increased cellularity, extracellular free water, fibrosis, glycogen, fat, and metal deposition [6]. Meanwhile, the development of a computer-aided diagnostic system that reduces the burden on radiologists and maintains the quality of service has been attempted on a number of occasions [7–9]. Although expectations of computer-aided diagnostic systems are high, only a few

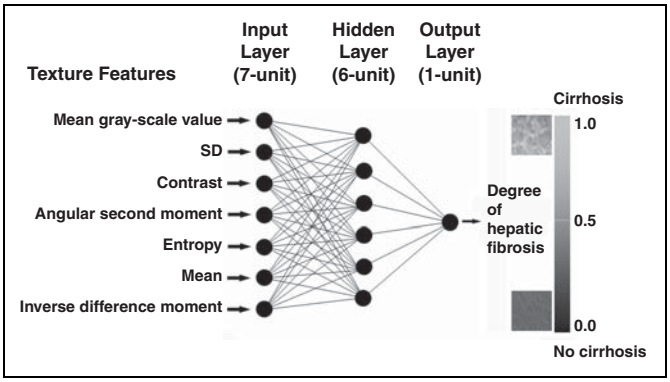

Fig. 1—Scheme shows texture feature analysis performed by artificial neural network program with three-layer learning algorithm of back propagation comprising seven-unit input layer, six-unit hidden layer, and one-unit output layer. Seven numeric parameters by finite difference method in 10 regions of interest placed in liver parenchyma were inputted into artificial neural network program, and probability value for presence of hepatic fibrosis in region of interest was outputted as continuous number between 0 (absent) and 1 (present).

articles on computer-aided diagnosis for the evaluation of hepatic fibrosis or cirrhosis by CT or sonography [10, 11] have been published, and few articles on MRI of these subjects are available. We performed a preliminary study of the diagnostic performance of a computer algorithm we developed for the MR-based diagnosis of hepatic fibrosis.

Materials and Methods

Patients

The institutional review board at Gifu University Hospital did not require approval, and the need for patient informed consent was waived because this was a retrospective study that used patient data and records obtained from routine clinical and radiologic practice. By searching our patient database, we identified 60 consecutive patients who underwent partial hepatectomy for a malignant hepatic tumor between February 2000 and January 2002. Of these, 52 underwent gadolinium-enhanced MRI for the preoperative evaluation of hepatic tumors at the department of radiology within 2 weeks of surgery. The liver diseases were hepatocellular carcinoma in chronic viral hepatitis type C or type B in 20 patients, hepatocellular carcinoma in cirrhosis in 20, cholangiocellular carcinoma in three, and liver metastasis in nine patients.

MRI

All MR images were obtained in the axial plane with a section thickness of 8–10 mm, a 2- to 3-mm intersection gap, and a field of view of 22 × 29–26 × 35 cm, which covered the whole liver, using a superconducting imager operating at 1.5 T (Signa Horizon, GE Healthcare) with a phased-array body coil. The imaging protocol comprised breath-hold T1-weighted spoiled gradient-recalled echo (GRE) (TR/TE, 150/1.6; matrix, 512 × 224 [number of frequency × phase encoding]; flip angle, 90°; signal acquisition, 1; slices, 18 per 26-second acquisition time), respiratory-triggered T2-weighted fast spin-echo (effective TR range/TE range, 3,333–8,571/77–80; matrix, 512 × 256; echo-train length, 8–18; signals acquired, 3–4; slices, 20 per 3.2- to 5.0-minute acquisition time), and gadolinium-enhanced triple-phase T1-weighted spoiled GRE (150/1.6; matrix, 512 × 224; flip angle, 90°; signal acquisition, 1; slices, 18 per 26-second acquisition time) sequences.

Gadolinium-enhanced GRE images were obtained after an antecubital IV bolus injection of 0.1 mmol/kg of gadopentetate dimeglumine (Magnevist, Schering) followed by a 20-mL sterile saline flush. Scanning delays for the hepatic arterial dominant, portal venous, and equilibrium phases were 18 seconds, 60 seconds, and 3 minutes, respectively, after initiating the contrast material injection. The chemical shift selective fat-saturation technique was not used because the acquisition time and number of slices were traded.

Pathologic Evaluation

A pathologist who was blinded to patient history and radiology and surgery reports retrospectively reviewed formalin-fixed slides of surgical specimens to evaluate the degree of hepatic fibrosis in nontumorous liver parenchyma using the 5-point Desmet scale: F0 indicates no fibrosis; F1, mild fibrosis; F2, moderate fibrosis; F3, severe fibrosis; and F4, cirrhosis [12].

Computer Algorithm Analysis

On a DICOM image of each MR sequence, a radiologist (unaware of patient information and the pathologic diagnosis) placed 10 square regions of interest (ROIs), each consisting of 32 × 32 pixels on the liver parenchyma, but avoiding large blood vessels, focal hepatic lesions, and prominent hepatic artifacts. A total of 10 ROIs were placed in the liver parenchyma devoid of large blood vessels and artifacts: eight in the right lobe (typically, two each in segments V, VI, VII, and VIII) and two in the left lobe (typically one each in segments II and III). In each ROI, texture features using the finite difference method were obtained as seven numeric values: mean gray-scale value, SD, contrast, angular second moment, entropy, mean, and inverse difference moment [13] (Appendix 1).

The texture features were further processed by an artificial neural network program containing a three-layer learning algorithm of the back propagation, comprising a seven-unit input layer, a six-unit hidden layer, and a one-unit output layer [14] (Fig. 1). The seven numeric parameters by the finite difference method in each ROI were entered into the artificial neural network program, and a probability value for the presence of hepatic fibrosis in an ROI was outputted as a continuous number between 0 (absent) and 1 (present). The 10 probability values of the 10 ROIs were averaged, and the overall average value obtained was used as the total probability value for the presence of hepatic fibrosis. MR images in eight patients (four with no fibrosis [F0] and four with cirrhosis [F4]) were used for training the artificial neural network program. MR images in the remaining 44 patients (three with no fibrosis [F0], 10 with mild fibrosis [F1], 15 with moderate fibrosis [F2], 13 with severe fibrosis [F3], and three with cirrhosis [F4]) were then used to evaluate the computer algorithm.

Radiologists' Interpretations

A study coordinator, an author with 5 years of posttraining experience in interpreting body MR images, prepared the MR images for review on a commercially available DICOM viewer; and two independent gastrointestinal radiologists with 15 and 7 years of posttraining experience at interpreting body MR images, who were unaware of patient history and radiology and surgery report details, reviewed the MR images in 44 patients for the presence of hepatic fibrosis. When a disagreement occurred, consensus was reached by discussion. All sequences—that is, T1-weighted, T2-weighted, hepatic arterial dominant phase, portal venous phase, equilibrium phase, combination unenhanced T1- and T2-weighted (unenhanced images combined), and all combination images (all images combined)—were reviewed in a randomized fashion.

MR images were magnified on the viewer frame to an appropriate degree so that only liver parenchymal textures were evaluated and liver contours were hidden to exclude the influence of

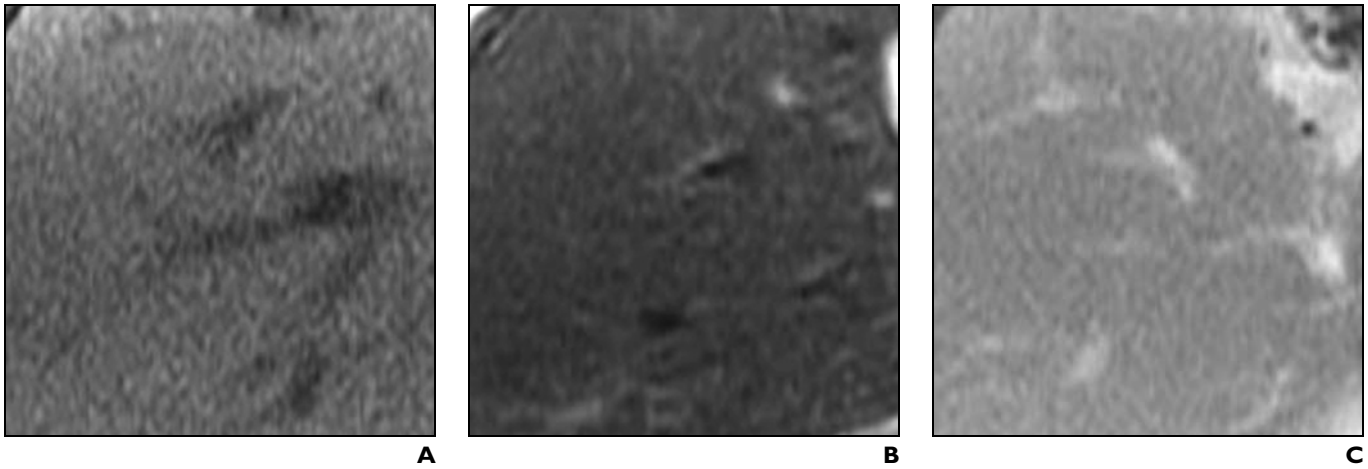

Fig. 2—73-year-old man without hepatitis (F0 on Desmet scale [1]) who underwent partial hepatectomy for solitary liver metastasis from ascending colon cancer.
A–C, T1-weighted spoiled gradient-recalled echo axial image (TR/TE, 150/1.6) (**A**), T2-weighted fast spin-echo axial image (4,286/80) (**B**), and gadolinium-enhanced equilibrium phase axial image (150/1.6) (**C**) show homogeneous signal intensity in liver parenchyma.

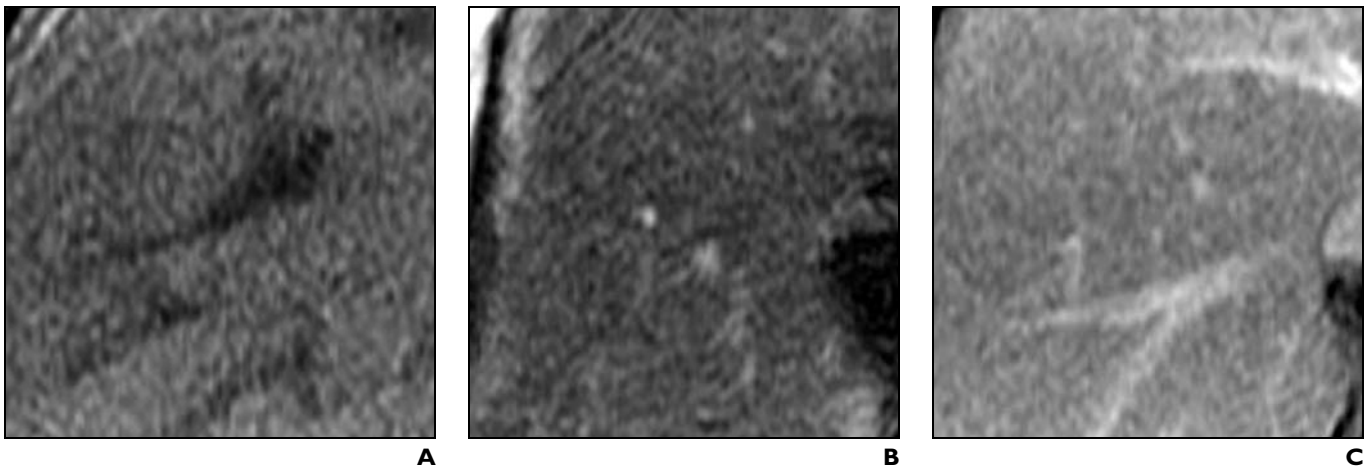

Fig. 3—76-year-old man with chronic type-B hepatitis and cirrhosis (F4 on Desmet scale [1]) who underwent partial hepatectomy for solitary hepatocellular carcinoma.
A and **B,** T1-weighted spoiled gradient-recalled echo axial image (TR/TE, 150/1.6) (**A**) and T2-weighted fast spin-echo axial image (4,286/80) (**B**) show tiny hypointense nodules, presumably corresponding to regenerative nodules in cirrhosis.
C, Gadolinium-enhanced equilibrium phase axial image (150/1.6) shows reticular pattern of enhancement in liver parenchyma that is presumably due to hepatic fibrosis.

liver configuration findings (Figs. 2 and 3). The radiologists on the DICOM viewer paged and reviewed only a few images at the middle level of the liver, taking care not to see the liver contours. After reviewing the MRI textures in the right and left lobes of the liver, a confidence level for the presence of fibrosis was assigned using a 4-point scale (1, definitely absent; 2, probably absent; 3, probably present; and 4, definitely present) for each sequence in a patient. The radiologists assigned confidence levels for the presence of hepatic fibrosis, paying attention to the degree of reticulonodular pattern of liver parenchymal textures on MR images that reflected pathologic characteristics of cirrhosis: fibrotic tissue surrounding regenerative nodules.

Statistical Analysis

Multiple regression analysis was used to examine correlations between the seven numeric values of texture features by the finite difference method and the pathologic degree of hepatic fibrosis. Receiver operating characteristic (ROC) curve analysis, in LABMRMC 1.0B software (Metz CE), was used to determine observer performances for the detection of hepatic fibrosis. For this analysis, the total probability for the presence of fibrosis determined by the computer algorithm, confidence levels for the presence of fibrosis determined by the radiologists' interpretations, and pathologic grades (F0–F2 were assumed to be actually negative, and F3 and F4, actually positive) were entered. Spearman's rank correlation coefficients were calculated to correlate computer algorithm output values and the radiologists' confidence levels for the presence of hepatic fibrosis with the pathologic fibrosis grades. Interobserver variability was assessed using kappa statistics.

Results

The correlation coefficients between the seven numeric values of texture features and the pathologic grades for hepatic fibrosis are summarized in Table 1. Mean gray values on T2-weighted images were found to be only weakly correlated with pathologic fibrosis grades ($r = 0.318$, $p < 0.05$).

Values for areas under the ROC curves (A_z) are summarized in Table 2. By the computer algorithm, the A_z value was greater for equi-

TABLE 1: Correlation Coefficients for the Seven Numeric Values by the Finite Difference Method and the Pathologic Degree of Hepatic Fibrosis

MRI Sequence	Mean Gray Value	SD	Contrast	Angular Second Moment	Entropy	Mean	Inverse Difference Moment
T1-weighted	0.158[a]	0.154	0.148	0.111	0.109	0.140	0.120
T2-weighted	0.318[b]	0.236	0.233	0.305	0.322	0.278	0.288
Hepatic arterial phase	0.143	0.156	0.162	0.154	0.185[b]	0.157	0.157
Portal venous phase	0.247[a]	0.227	0.225	0.227	0.210	0.232	0.231
Equilibrium phase	0.282	0.257	0.258	0.290	0.294	0.281	0.284

[a] p between 0.05 and 0.1.
[b] $p < 0.05$.

TABLE 2: Area Under the Curve (A_z) Values with Computer Algorithm Analysis and Radiologists' Interpretations for Detection of Hepatic Fibrosis

Method	A_z
Computer algorithm analysis	
T1-weighted	0.597
T2-weighted	0.525
Hepatic arterial phase	0.624
Portal venous phase	0.699
Equilibrium phase	0.801[a]
Interpretation by radiologists	
T1-weighted	0.630
T2-weighted	0.645
Hepatic arterial phase	0.539
Portal venous phase	0.503
Equilibrium phase	0.546
Unenhanced images combined	0.655
All images combined	0.715[b]

[a] Greater than with T1-weighted and T2-weighted images of computer algorithm analysis and greater than with equilibrium phase images of radiologists' interpretation ($p < 0.05$).
[b] Greater than with portal venous phase images with radiologists interpretation ($p < 0.05$).

librium phase images ($A_z = 0.801$) than for T1-weighted ($A_z = 0.597$) or T2-weighted ($A_z = 0.525$) images ($p < 0.05$). By the radiologists' interpretations, the A_z value for all images combined ($A_z = 0.715$) was greater than that of the portal venous phase images ($A_z = 0.503$) ($p < 0.05$). The A_z value for equilibrium phase images in the computer algorithm ($A_z = 0.801$) was greater than for equilibrium phase images of radiologists ($A_z = 0.546$).

Correlation coefficients of the total probability determined by the computer algorithm and the confidence levels determined by radiologists with pathologic grades are summarized in Table 3. By the computer algorithm, the outputs of T1-weighted ($r = 0.329$, $p = 0.031$) and portal venous phase ($r = 0.308$, $p = 0.044$) images were weakly correlated and those of equilibrium phase images showed a moderate correlation ($r = 0.502$, $p = 0.001$) with the pathologic grades. By the radiologists' interpretations, the confidence levels of unenhanced images combined were weakly correlated ($r = 0.357$, $p = 0.019$) and those of all images combined were moderately correlated ($r = 0.473$, $p = 0.002$) with pathologic grades.

The kappa values for the two radiologists who independently rated images ranged from 0.62 to 0.80 (mean, $\kappa = 0.71$), indicating substantial agreement.

Discussion

Of the seven numeric values of texture features, only the mean gray-scale value of T2-weighted images was found to be weakly correlated with the pathologic degree of hepatic fibrosis by multiple regression analysis. We inferred that this was because the mean gray-scale value was the average of pixel values reflecting the brightness of ROI, and the signal intensity of the liver parenchyma might decrease on T2-weighted images because of regenerative nodules in cirrhosis or possible hemosiderin deposition [15, 16].

According to the radiologists' interpretations, correlation coefficients and A_z values were increased by interpreting both unenhanced T1- and T2-weighted images. This was presumably because the reticular patterns of hepatic fibrosis and regenerative nodules in cirrhosis were more efficiently recognized by radiologists after combination interpretation. Hepatic fibrosis, which often harbors vascular spaces, was observed as isointense or slightly hypointense on T1-weighted images and as slightly hyperintense on T2-weighted images because of increased levels of free water in fibrotic tissue. Moreover, regenerative nodules with possible hemosiderin deposition might show discrete hypointensity on T2-weighted images [15, 16].

Correlation coefficients and A_z values were greatest with contrast-enhanced equilibrium phase images by the computer algorithm, whereas the values of equilibrium phase images by the radiologists' interpretations were not so high. We infer that the fibrotic tissue surrounding regenerative nodules showed reticular hyperintensity due to delayed enhancement on gadolinium-enhanced equilibrium phase images, and that the reticular enhancement pattern was better recognized by the computer algorithm than by the radiologists. Although radiologists can often detect the reticular enhancement of hepatic fibrosis, radiologists' performance was significantly lower than that of the computer algorithm.

We masked liver contours from the radiologists as well as information on hepatic configurations, such as enlargement or shrinking of liver segments and irregular liver surfaces. However, radiologists in the clinical setting interpret hepatic parenchymal textures and configurations simultaneously to determine the degree of cirrhosis. Thus, if the radiologists had been able to observe the whole liver on multiple-sequence images in our study, their performance at diagnosing hepatic fibrosis would probably have improved. Therefore, our finding that the diagnostic performance of the computer algorithm with equilibrium phase images was high may indicate that the computer algorithm could be used as a simple measurement tool for evaluating hepatic parenchymal textures and could aid in the diagnosis of hepatic fibrosis.

We included MR images of patients who underwent partial hepatectomy; the study cohort did not include cases of severe cirrhosis with highly impaired hepatic functional reserve. If our study had included a number of patients with severe fibrosis or cirrhosis, our results by ROC analysis and correlation might have been improved. Severe cirrhosis is often visualized as numerous regenerative nodules and as a reticular fibrotic pattern on MR images, and thus the diagnosis of severe hepatic fibrosis is not difficult. However, the diagnosis of hepatic fibrosis of an intermediate degree may not be easy because hepatic parenchymal textural alterations (due to regenerative nodules and fibrosis in such livers) are too subtle to convince radiologists of the presence of disease. Regarding the detection and grading of hepatic fibrosis of a moderate or lesser degree, the computer

TABLE 3: Correlation of Computer Algorithm Analysis and Radiologists' Interpretation with Pathologic Degree of Hepatic Fibrosis

Method	Correlation Coefficient (*r*)	*p*
Computer algorithm analysis		
T1-weighted	0.329	0.031[a]
T2-weighted	–0.006	0.967
Hepatic arterial phase	0.259	0.090
Portal venous phase	0.308	0.044[a]
Equilibrium phase	0.502	0.001[a]
Interpretation by radiologists		
T1-weighted	0.238	0.119
T2-weighted	0.270	0.077
Hepatic arterial phase	0.136	0.372
Portal venous phase	0.128	0.401
Equilibrium phase	0.172	0.259
Unenhanced images combined	0.357	0.019[a]
All images combined	0.473	0.002[a]

[a]Significant correlation with pathologic degree of hepatic fibrosis.

algorithm proved superior to the radiologists' interpretations in our study.

We did not find strong correlations between pathologic fibrosis grades and outputs by computer algorithm or by radiologists, and we inferred some possible limitations in our study methods: We adopted only one pathologic parameter of fibrosis among a variety of factors in the pathologic diagnosis of chronic hepatitis or cirrhosis, such as periportal necrosis, intralobular necrosis, and portal inflammation [17]. Although the radiologists assessed hepatic fibrosis, paying attention to the reticulonodular pattern indicating fibrotic tissue surrounding regenerative nodules, sizes of regenerative nodules and thickness of fibrosis vary in individual patients, depending on the kind of underlying diseases. We did not include patients with severe cirrhosis because such patients could not undergo surgical treatment for liver tumors. The pathologist evaluated liver parenchyma near hepatic tumors that were surgically resected, whereas the two radiologists reviewed a few MR images at the middle level of the liver: Liver parenchyma evaluated by the pathologist and the radiologists did not necessarily match, and such a difference might have yielded some correlation errors because hepatic fibrosis does not occur evenly in the liver.

Our study has several other limitations. The study population was small because the study was conducted in a single institution. A multiinstitutional study of a program with a more user-friendly interface may be warranted to determine the true clinical impact. Although the radiologists gave diagnoses referring to multiple sequences, the computer algorithm processed images by a single sequence. Thus, we need to develop computer algorithms that process multiple sequences in combination. We used a non–fat-suppressed 2D GRE sequence for the gadolinium-enhanced study because that was the only sequence available as a result of the limited performance of our MR imager at that time. Recently, a variety of 3D GRE sequences allowing acquisitions of thin slices have been available for gadolinium-enhanced studies, and we have been using such sequences. Nevertheless, we believe that the MR images in our study exhibited fine textures of liver parenchyma because we used high imaging matrices (512 × 224).

In conclusion, this texture analysis of MR images of the liver using the finite difference method and an artificial neural network reflected the degree of hepatic fibrosis, and equilibrium phase images were found to be most suitable for analytic purposes. Our study indicates that MR image texture analysis using suitable computer algorithms offers the potential for predicting the degree of hepatic fibrosis.

Acknowledgments

The contribution of Noriyuki Moriyama, Research Center for Cancer Prevention and Screening, National Cancer Center Hospital, Tokyo, Japan, to our research is greatly appreciated. We thank Wenguang Li, Tetsuji Tajima, and Takeshi Hara, Department of Information Science, Faculty of Engineering, Gifu University, Gifu, Japan, for providing helpful technical support and for performing many of the tasks associated with this project.

References

1. El-Serag HB, Davila JA, Petersen NJ, et al. The continuing increase in the incidence of hepatocellular carcinoma in the United States: an update. *Ann Intern Med* 2003; 139:817–823
2. El-Serag HB, Mason AC. Rising incidence of hepatocellular carcinoma in the United States. *N Engl J Med* 1999; 340:745–750
3. Benvegnu L, Gios M, Boccato S, Alberti A. Natural history of compensated viral cirrhosis: a prospective study on the incidence and hierarchy of major complications. *Gut* 2004; 53:744–749
4. Yatsuhashi H, Yano M. Natural history of chronic hepatitis C. *J Gastroenterol Hepatol* 2000; 15:111–116
5. Tokita H, Fukui H, Tanaka A, et al. Risk factors for the development of hepatocellular carcinoma among patients with chronic hepatitis C who achieved a sustained virological response to interferon therapy. *J Gastroenterol Hepatol* 2005; 20:752–758
6. Bartolozzi C, Cioni D, Donati F, Lencioni R. Focal liver lesions: MR imaging–pathologic correlation. *Eur Radiol* 2001; 11:1374–1388
7. Jiang Y, Nishikawa RM, Schmidt RA, Toledano AY, Doi K. Potential of computer-aided diagnosis to reduce variability in radiologists' interpretations of mammograms depicting microcalcifications. *Radiology* 2001; 220:787–794
8. Chan HP, Doi K, Vyborny CJ, et al. Improvement in radiologists' detection of clustered microcalcifications on mammograms: the potential of computer-aided diagnosis. *Invest Radiol* 1990; 25:1102–1110
9. Doi K, MacMahon H, Katsuragawa S, Nishikawa RM, Jiang Y. Computer-aided diagnosis in radiology: potential and pitfalls. *Eur J Radiol* 1999; 31:97–109
10. Wang Y, Ito K, Taniguchi N, et al. Studies on tissue characterization by texture analysis with co-occurrence matrix method using ultrasonography and CT imaging. *J Med Ultrasonics* 2002; 29:211–223
11. Awaya H, Mitchell DG, Kamishima T, Holland G, Ito K, Matsumoto T. Cirrhosis: modified caudate–right lobe ratio. *Radiology* 2002; 224:769–774
12. Desmet VJ, Gerber M, Hoofnagle JH, Manns M, Scheuer PJ. Classification of chronic hepatitis: diagnosis, grading and staging. *Hepatology* 1994; 19:1513–1520
13. Haralick RM, Shanmugam K, Dinstein I. Texture features for image classification. *IEEE Trans Sys*

Man Cybern 1973; SMC-3-6:610–621

14. Rumelhart DE, McClellend JL. Learning representations by back-propagating errors. *Nature* 1986; 323:533–536
15. Itai Y, Ohnishi S, Ohtomo K, et al. Regenerating nodules of liver cirrhosis: MR imaging. *Radiology* 1987; 165:419–423
16. Ohtomo K, Itai Y, Ohtomo Y, Shiga J, Iio M. Regenerating nodules of liver cirrhosis: MR imaging with pathologic correlation. *AJR* 1990; 154:505–507
17. Knodell RG, Ishak KG, Black WC, et al. Formulation and application of a numerical scoring system for assessing histological activity in asymptomatic chronic active hepatitis. *Hepatology* 1981; 1:431–435

APPENDIX 1: Texture Features for the Finite Difference Method

The seven features used for texture analysis were derived from the finite difference method and the histogram; they have been used for the standard evaluation of images to extract texture features [10]. Of the seven, five (contrast, angular second moment, entropy, mean, inverse difference moment) were derived from the gray-level difference method and another two (mean gray-scale value, SD), from the basic image features by histogram analysis.

Among the five features by the finite difference method, "contrast" is the difference moment of the matrix and is a measure of local variations present in the image. Contrast also measures the spread of matrix values. A low contrast value reflects uniformly gray images; conversely, high-contrast images show much local variation. "Angular second moment" is a measure of the textural uniformity of an image. When entries in the co-occurrence matrix are equal, this has a low value. Moreover, this measure is higher when some entries are high and others are low. If an image has a uniform gray level, there will be only one entry in the co-occurrence matrix, and this will produce the highest value for the angular second moment. "Entropy" is a measure of the randomness of the image texture. When the spatial co-occurrence matrix is equal, entropy is the highest. Entropy is at a minimum when the elements in a matrix are very unequal. Hence, higher values for entropy indicate greater randomness in the image. "Mean" is the average value in the probabilities function, and "inverse difference moment" measures image homogeneity.

Regarding the two features by histogram analysis, "mean gray-scale value" is defined as the average pixel value in a region of interest (ROI) and indicates the intensity or brightness of a region. For example, a value of 255 is very bright and a value of 0, very dark. "Standard deviation" indicates variation from the mean gray-scale value. If an ROI is homogeneous, the SD is small; if the region is heterogeneous, the SD is large. The mean and the inverse difference moment by the finite difference method are similar to the mean gray-scale value and SD by histogram analysis. The mean and inverse difference moment are calculated using second-order statistics, whereas the mean gray-scale value and SD are calculated using first-order statistics.